ARMY RESEARCH LABORATORY

Efficient Determination of Hugoniot States Using Classical Molecular Simulation Techniques

by John K. Brennan and Betsy M. Rice

ARL-RP-145 **September 2006**

A reprint from *Molecular Physics*, vol. 101, no. 22, pp. 3309–3322, 20 November 2003.

Reprinted with permission from *Molecular Physics*. Copyright 2005, Taylor & Francis Group Ltd. http://www.tandf.co.uk/journals.

Approved for public release; distribution is unlimited.

NOTICES

Disclaimers

The findings in this report are not to be construed as an official Department of the Army position unless so designated by other authorized documents.

Citation of manufacturer's or trade names does not constitute an official endorsement or approval of the use thereof.

Destroy this report when it is no longer needed. Do not return it to the originator.

Army Research Laboratory

Aberdeen Proving Ground, MD 21005-5066

ARL-RP-145 **September 2006**

Efficient Determination of Hugoniot States Using Classical Molecular Simulation Techniques

John K. Brennan and Betsy M. Rice
Weapons and Materials Research Directorate, ARL

A reprint from *Molecular Physics*, vol. 101, no. 22, pp. 3309–3322, 20 November 2003.

Reprinted with permission from *Molecular Physics*. Copyright 2005, Taylor & Francis Group Ltd. http://www.tandf.co.uk/journals.

Approved for public release; distribution is unlimited.

REPORT DOCUMENTATION PAGE

Form Approved
OMB No. 0704-0188

Public reporting burden for this collection of information is estimated to average 1 hour per response, including the time for reviewing instructions, searching existing data sources, gathering and maintaining the data needed, and completing and reviewing the collection information. Send comments regarding this burden estimate or any other aspect of this collection of information, including suggestions for reducing the burden, to Department of Defense, Washington Headquarters Services, Directorate for Information Operations and Reports (0704-0188), 1215 Jefferson Davis Highway, Suite 1204, Arlington, VA 22202-4302. Respondents should be aware that notwithstanding any other provision of law, no person shall be subject to any penalty for failing to comply with a collection of information if it does not display a currently valid OMB control number.
PLEASE DO NOT RETURN YOUR FORM TO THE ABOVE ADDRESS.

1. REPORT DATE *(DD-MM-YYYY)*	2. REPORT TYPE	3. DATES COVERED (From - To)
September 2006	Reprint	May 2003–December 2003

4. TITLE AND SUBTITLE
Efficient Determination of Hugoniot States Using Classical Molecular Simulation Techniques

5a. CONTRACT NUMBER

5b. GRANT NUMBER

5c. PROGRAM ELEMENT NUMBER

6. AUTHOR(S)
John K. Brennan and Betsy M. Rice

5d. PROJECT NUMBER
H4311

5e. TASK NUMBER

5f. WORK UNIT NUMBER

7. PERFORMING ORGANIZATION NAME(S) AND ADDRESS(ES)
U.S. Army Research Laboratory
ATTN: AMSRD-ARL-WM-BD
Aberdeen Proving Ground, MD 21005-5066

8. PERFORMING ORGANIZATION REPORT NUMBER
ARL-RP-145

9. SPONSORING/MONITORING AGENCY NAME(S) AND ADDRESS(ES)

10. SPONSOR/MONITOR'S ACRONYM(S)

11. SPONSOR/MONITOR'S REPORT NUMBER(S)

12. DISTRIBUTION/AVAILABILITY STATEMENT
Approved for public release; distribution is unlimited.

13. SUPPLEMENTARY NOTES
A reprint from *Molecular Physics*, vol. 101, no. 22, pp. 3309–3322, 20 November 2003.

14. ABSTRACT
We present a methodology for the efficient calculation of the shock Hugoniot using standard molecular simulation techniques. The method is an extension of an equation of state methodology proposed by Erpenbeck [1992, *Phys. Rev.* A, **46**, 6406] and is considered as an alternative to other methods that generate Hugoniot properties. We illustrate the methodology for shocked liquid N_2 using two different simulation methods: (a) the reactive Monte Carlo method for a reactive system; and (b) the molecular dynamics method for a non-reactive system. The method is shown to be accurate, stable and generally independent of the algorithm parameters. We find excellent agreement with results calculated by other previous simulation studies. The results show that the methodology provides a simulation tool capable of determining points on the shock Hugoniot from a single simulation in an efficient, straightforward manner. Further applications and extensions of the method are briefly discussed.

15. SUBJECT TERMS
molecular simulation, Monte Carlo, reaction ensemble

16. SECURITY CLASSIFICATION OF:			17. LIMITATION OF ABSTRACT	18. NUMBER OF PAGES	19a. NAME OF RESPONSIBLE PERSON
					John K. Brennan
a. REPORT	b. ABSTRACT	c. THIS PAGE			19b. TELEPHONE NUMBER (*Include area code*)
UNCLASSIFIED	UNCLASSIFIED	UNCLASSIFIED	UL	20	410-306-0678

Standard Form 298 (Rev. 8/98)
Prescribed by ANSI Std. Z39.18

MOLECULAR PHYSICS, 20 NOVEMBER 2003, VOL. 101, NO. 22, 3309–3322

Taylor & Francis
Taylor & Francis Group

Efficient determination of Hugoniot states using classical molecular simulation techniques

JOHN K. BRENNAN* and BETSY M. RICE

Weapons and Materials Research Directorate, US Army Research Laboratory, Aberdeen Proving Ground, MD 21005-5066, USA

(*Received 13 June 2003; accepted 12 October 2003*)

We present a methodology for the efficient calculation of the shock Hugoniot using standard molecular simulation techniques. The method is an extension of an equation of state methodology proposed by Erpenbeck [1992, *Phys. Rev.* A, **46,** 6406] and is considered as an alternative to other methods that generate Hugoniot properties. We illustrate the methodology for shocked liquid N_2 using two different simulation methods: (a) the reactive Monte Carlo method for a reactive system; and (b) the molecular dynamics method for a non-reactive system. The method is shown to be accurate, stable and generally independent of the algorithm parameters. We find excellent agreement with results calculated by other previous simulation studies. The results show that the methodology provides a simulation tool capable of determining points on the shock Hugoniot from a single simulation in an efficient, straightforward manner. Further applications and extensions of the method are briefly discussed.

1. Introduction

The behaviour of materials under conditions of extreme temperature and pressure is of significant interest in many fields of physics and fluid science [1–4]. Of special interest are energetic materials, a class of materials of critical industrial and military importance. These materials exhibit chemically and physically interesting behaviour when exposed to extreme temperatures and pressures. In particular, when subjected to shock, energetic materials often undergo rapid reactions that produce a heterogeneous mixture of chemical species that are accompanied by huge energy releases and can produce pressures up to several hundred GPa and temperatures exceeding 10 000 K. For a sufficiently strong shock, a supersonic, self-propagating reaction wave known as a detonation can be initiated. Unfortunately, the extreme conditions along with the short time and length scales over which a detonation occurs poses considerable experimental challenges in characterizing the material behind the detonation front. Therefore a concerted effort, which combines experimental, theoretical and simulation approaches, is essential for furthering our understanding of such shocked systems. Advances in experimental capabilities provide us with crucial property data, while the continuing development of accurate equations of state has allowed reasonable predictions of various shock properties [5, 6]. Similarly, the development of novel methods to simulate these complex systems has been the focus of research efforts and has recently led to the invention of some uniquely effective simulation tools [7–4]. These classical simulation methods can be implemented irrespective of rate limitations, the production of huge energy releases, or extreme thermodynamic conditions.

The *Hugoniot* curve, a commonly calculated property in shock and detonation science, reveals many properties of shocked materials and knowledge of which is critical to the design of new materials and application platforms. This curve consists of the set of (PVT) points for which the Hugoniot expression,

$$H_g = E - E_o - \tfrac{1}{2}(P + P_o)(V_o - V), \qquad (1)$$

is zero. In equation (1), E is the specific internal energy, P is the pressure and $V = 1/\rho$ is the specific volume (ρ is the specific density). The term *specific* refers to the quantity per unit mass, while the subscript 'o' refers to the quantity in the initial unshocked state.

Presently, three approaches exist for calculating the shock Hugoniot states from classical molecular simulation, each with their own advantages and disadvantages. The first approach, which we term here the Erpenbeck equation of state method (E-EOS), is the most indirect of the approaches. The original version of the method involves performing several separate simulations at appropriately chosen temperatures and pressures. Each

*Author for correspondence. e-mail: jbrennan@arl.army.mil

Molecular Physics ISSN 0026–8976 print/ISSN 1362–3028 online © 2003 Taylor & Francis Ltd
http://www.tandf.co.uk/journals
DOI: 10.1080/00268970310001636404

simulation generates an equation of state point for subsequent evaluation of the Hugoniot expression followed by interpolation to locate the point at which the expression is zero. The molecular dynamics (MD) method has been implemented in the Erpenbeck approach using reactive potentials that mimic chemical bond breaking and forming between species [12, 13].

An approach for calculating the shock Hugoniot properties from classical molecular simulation that is more direct than the E-EOS method is the piston-driven molecular dynamics method [7, 8]. Piston-driven MD generates a point on the Hugoniot curve from a single simulation, thus avoiding the need to calculate several EOS points (as in the E-EOS approach) in order to obtain the desired result. The method mimics the laboratory system by calculating properties behind the shock discontinuity in a shock wave simulation. Shock waves are produced by hitting the free edge of the molecular solid with a rigid layer of atoms that are moving at a constant velocity. Different shocked states are obtained by starting with different initial piston velocities [8].

A third approach, termed the uniaxial Hugoniostat method [9], is a molecular dynamics method which utilizes modified equations of motion that constrain the system to states that correspond to points on the shock Hugoniot curve. This method is computationally more efficient than both MD implementations of the E-EOS method and the piston-driven shock wave simulations. The E-EOS method requires a system of only a few hundred atoms (with periodic boundary conditions imposed), but several simulations are required to generate a single shock Hugoniot point. The piston-driven MD method will produce results from a single simulation. However, the system size must be sufficiently large so that the properties behind the propagating shock wave can be averaged over time. The uniaxial Hugoniostat method, on the other hand, can generate a point on the Hugoniot curve from a single simulation whose system size is relatively small.

Unfortunately, none of these MD methods can be applied to the calculation of the shock Hugoniot locus over a wide range of temperatures and pressures unless certain conditions are fulfilled. Most energetic materials respond to shock by decomposing into a complex (sometimes heterogeneous) mixture of many different chemical species. Thus, for these multi-component systems, the implementation of the uniaxial Hugoniostat method, the MD E-EOS method or the piston-driven MD method requires either: (1) *a priori* knowledge of the relative concentrations of each chemical species in the shocked state; or (2) a reactive potential that simulates bond breaking and bond formation. Typically, the relative species concentrations of the shocked state are lacking; moreover, knowledge of these quantities is desired. Furthermore, although significant advances have been made in developing reactive potentials for shocked materials, the potentials are presently limited to idealized representations of the chemistry that occurs [13–26]. The most accurate interaction potentials for energetic materials available at this time are all non-reactive [27–41].

Monte Carlo methodologies circumvent some of the restrictions associated with the MD methods for calculating shock Hugoniot states. The reactive Monte Carlo method (RxMC) [10] and the composite Monte Carlo method [11] have both been used to calculate Hugoniot properties through the E-EOS approach. These two closely related methods do not require a reactive potential or *a priori* knowledge of species concentrations for each Hugoniot state. They also do not require the specification of species chemical potentials or chemical potential differences to determine chemical equilibrium states of the reactive mixtures. Both methods have been applied to simple, spherically-averaged intermolecular potentials [10, 11] but can readily be applied to complex potentials that include multi-site and/or electrically-charged species as well as multi-phase mixtures. Therefore, in the absence of reactive potentials or *a priori* knowledge of species concentrations, the only applicable approaches for simulating the Hugoniot properties of a shocked material are the Erpenbeck EOS method performed using either the RxMC or composite MC methods.

As previously mentioned, however, the original E-EOS method requires simulations of several equation of state points to generate a single point on the shock Hugoniot curve. Each separate simulation requires sufficient equilibration and data collection steps. In an effort to reduce the number of steps and to minimize associated computational costs, we have implemented a numerical approach within the framework of the E-EOS approach. The resulting method requires only a single simulation to determine a point on the Hugoniot curve. The fitting procedure used to determine the root of the Hugoniot expression ($H_g = 0$) in the original version of the E-EOS approach is replaced by an iterative numerical procedure built into the framework of the simulation.

A brief illustration of the method using isothermal–isobaric ensemble (NPT) simulations is given. The simulation is initiated at the specified temperature and pressure, and the Hugoniot expression is evaluated (using instantaneous values of V, P and E that depend only on the current configuration) at periodic intervals during the simulation run and accumulated for averaging. The averaged Hugoniot value is then used in a numerical root-finding algorithm (e.g. Newton–Raphson [42]) to provide an estimate of the Hugoniot pressure. The

imposed pressure for the simulation is subsequently changed to correspond to the new estimate of the Hugoniot pressure. The simulation continues using this new imposed pressure constraint. This process is repeated until the Hugoniot function converges to zero (more precisely, within a desired tolerance of zero). The value of the pressure and corresponding volume averaged over the entire simulation run characterize the Hugoniot state at that temperature.

The method is akin to the phase equilibria methods that utilize thermodynamic integration to determine coexistence behaviour [43–45]. In these calculations, a finite-difference algorithm is used to numerically integrate the differential equations, the Clausius–Clapeyron [43, 44] or the Gibbs–Duhem expressions [45], which govern the changes in thermodynamic parameters along the phase coexistence curve. Similarly, for the method introduced here, a numerical estimate of the root of the Hugoniot expression is made. Both approaches are iterated until the desired convergence has been reached.

In summary, we demonstrate the accuracy and stability of a method to calculate the shock Hugoniot properties of materials when implementing the E-EOS method either in an MD or RxMC framework. (Implementation of the modified E-EOS method using the composite MC method is analogous to the RxMC method and will not be demonstrated here.) The method, which we term the adaptive Erpenbeck equation of state method (AE-EOS), is intended to be a tool that is an alternative to the existing methodologies in order to overcome some of their limitations. We demonstrate the validity of the AE-EOS method for calculating the Hugoniot properties of liquid N_2 in the non-reactive regime using molecular dynamics and in the reactive regime using reactive Monte Carlo. The outline of the paper is as follows. The formalism and practical details of the methodology are presented in section 2. Applications of the method are given in section 3, while assessments of the results and possible extensions of the method are given in section 4.

2. Methodology

2.1. *Formalism*

The Hugoniot function $H_g = H_g[E, T, P(\text{or } V)]$, and so a search for $H_g = 0$ in the original Erpenbeck EOS method is implemented by fixing two independent variables in a simulation and calculating the remaining variable. For example, when simulating with an isothermal–isobaric ensemble, E is calculated from the simulation. Typically, several simulations must be performed using various choices of the independent variables to generate sufficient points so that the Hugoniot state can be obtained through interpolation. (Detailed outlines of the original E-EOS approach using the molecular dynamics and the RxMC methods can be found in [12] and [10], respectively.) The adaptive Erpenbeck equation of state method presented in this work eliminates the interpolation procedure by using a root-finding algorithm to determine $H_g = 0$. For example, the expression for finding the root of a function using the Newton–Raphson method is [42]

$$x_{n+1} = x_n - \frac{f(x_n)}{f'(x_n)}, \tag{2}$$

where $f'(x_n) = \mathrm{d}f(x_n)/\mathrm{d}x_n$, $f(x_n) = H_g$ and we choose either $x_n = E$, T or P (or V). The basis of the AE-EOS method is to begin a simulation at an initial x_n and after a prescribed number of simulation steps, the quantities $f(x_n)$ and $f'(x_n)$ are calculated and x_{n+1} is determined. The simulation continues using the predicted value x_{n+1}. This procedure is repeated until the results converge.

In the following, we demonstrate the AE-EOS method for P as the independent variable used to find the root of the Hugoniot function. (Considerations for choosing the other variables E, T and V as the independent quantity in the root-finding algorithm are presented in the Appendix.) The working expression for predicting the pressure of the Hugoniot state within the framework of the Newton–Raphson procedure (equation (2)) is then

$$P^{\text{predicted}} = P^{\text{current}} - \frac{H_g^{\text{current}}}{\mathrm{d}H_g^{\text{current}}/\mathrm{d}P}. \tag{3}$$

In the procedure presented here, the predicted pressure, $P^{\text{predicted}}$, is determined using averaged instantaneous values of the Hugoniot expression (equation (1)) and its derivative with respect to pressure, i.e. $H_g^{\text{current}} = \langle H_g \rangle$ and $\mathrm{d}H_g^{\text{current}}/\mathrm{d}P = \langle \mathrm{d}H_g/\mathrm{d}P \rangle$, where '$\langle\,\rangle$' denotes averages of instantaneous values. The instantaneous Hugoniot values (and derivatives) were determined using the corresponding instantaneous values of P, E and T generated during the simulation.

Next, since the internal energy can be written as [10]

$$E = \sum_{i=1}^{c_j} y_i H_i^{\text{o}} + U^{\text{conf}} - RT, \tag{4}$$

then equation (1) can be rewritten as

$$H_g = \left[\left(\sum_{i=1}^{c_j} y_i H_i^{\text{o}} + U^{\text{conf}} - RT \right) - E_0 \right] - \frac{1}{2}(PV_0 - PV + P_0V_0 - VP_0), \tag{5}$$

where E_0, P_0 and V_0 are the values of the initial state (and thus constant) and $U^{\text{conf}} = \sum_i \sum_{j>i} U_{ij}(r_{ij})$, where U_{ij}

is the pair potential energy [46]. All quantities in equations (4) and (5) are used here in the context of instantaneous quantities that depend only on the current configuration. The derivative term required in equation (3) is then

$$\left.\frac{\mathrm{d}H_{\mathrm{g}}}{\mathrm{d}P}\right|_V = \frac{\mathrm{d}}{\mathrm{d}P}\left(\sum_{i=1}^{c_j} y_i H_i^{\mathrm{o}}\right) + \frac{\mathrm{d}}{\mathrm{d}P}\left(U^{\mathrm{conf}}\right) - \frac{\mathrm{d}}{\mathrm{d}P}(RT) - \frac{1}{2}\frac{\mathrm{d}}{\mathrm{d}P}(PV_0 - PV + P_0V_0 - VP_0). \quad (6)$$

The first and third terms on the right-hand side of equation (6) are not functions of P and can be eliminated. Further since U^{conf} is calculated as an instantaneous value, $U^{\mathrm{conf}} = U^{\mathrm{conf}}(r)$ only and thus can be eliminated. Finally, the last term is readily solved, so that equation (6) reduces to

$$\frac{\mathrm{d}H_{\mathrm{g}}}{\mathrm{d}P} = \frac{1}{2}(V - V_0). \quad (7)$$

The algorithm for the adaptive Erpenbeck equation of state method with P chosen as the independent variable is as follows.

Step 1: Set the temperature for the Hugoniot state ($T_{H_{\mathrm{g}}}$).
Step 2: Guess the pressure for this Hugoniot state (P^{current}).
Step 3: Perform an isothermal–isobaric ensemble simulation (MD or RxMC) at $T_{H_{\mathrm{g}}}$ and P^{current}.
Step 4: After allowing the system to relax to P^{current}, accumulate instantaneous values of H_{g} and $\mathrm{d}H_{\mathrm{g}}/\mathrm{d}P$ during the simulation using equations (5) and (7), respectively.
Step 5: After a prescribed number of steps, calculate averaged values of H_{g} and $\mathrm{d}H_{\mathrm{g}}/\mathrm{d}P$ and predict the Hugoniot pressure using equation (3). (The averaged values of H_{g} and $\mathrm{d}H_{\mathrm{g}}/\mathrm{d}P$ can be determined by several methods, which are considered in the next section.)
Step 6: Repeat steps (3)–(6) until the results converge to the desired statistical uncertainty.

2.2. *Practical details*

Next, we consider a few practical details of implementing the AE-EOS method. Our intent is to generalize the method for implementation into any of the standard molecular simulation techniques (MD, RxMC or composite MC). We consider the effect of several parameters on the accuracy and stability of the method. Below we address these issues, the logic behind our choices and the trade-offs involved.

2.2.1. *Root-finding algorithm*

There exists a wide range of root-finding algorithms, including the Newton–Raphson method, the secant method, the bi-section method and Halley's method [42]. Newton–Raphson (equation (2)) is a rather straightforward method but can be unstable near a horizontal asymptote or local minimum. A similar algorithm is Halley's method which includes an additional term $(\mathrm{d}f'(x_n)/\mathrm{d}x_n)$ from the Taylor series in the derivation of the method. When the pressure is chosen as the independent variable, $\mathrm{d}^2H_{\mathrm{g}}/\mathrm{d}P^2 = 0$ (see equation (7)) so Halley's method reduces to the Newton–Raphson method. Another root-finding method is the secant method, which estimates the derivative term using $f'(x_n) = [f(x_n) - f(x_{n-1})]/(x_n - x_{n-1})$. However, use of the method in the AE-EOS method requires two recent points along the Hugoniot curve as opposed to only one for the Newton–Raphson method. Finally, if we can be certain that the solution of the Hugoniot expression lies within a known interval, then we can iteratively converge to the solution using the bi-section method. However, a balance must be established between statistical uncertainty and the desired convergence when implementing the bi-section method in a molecular simulation, since statistical fluctuations cannot be greater than the size of the interval. In an effort to keep the method proposed here as general and straightforward as possible, we have implemented the Newton–Raphson method. The well-known problems of this method near a local minimum or asymptote have not been encountered for the Hugoniot expression in this work as well as for other work [10, 12, 13], but one should be mindful of its limitations.

2.2.2. *Initial guess of pressure*

In any molecular simulation, it is necessary to design a starting configuration so that the relaxed system is physically reasonable and computationally consistent. For example, consider an isothermal–isobaric ensemble simulation where periodic boundaries are imposed and where the potential energy function has a limited interaction range. In such a case, an appropriate number of molecules must be chosen so that the relaxed box size is consistent with the minimum image convention, i.e. one-half the box size must be greater than or equal to the potential cut-off distance [46]. Similarly, appropriate starting conditions for the AE-EOS method are required, particularly for the initial guess of the imposed pressure. Since the converged result (i.e. $H_{\mathrm{g}} = 0$) will produce a Hugoniot pressure that is equal to the imposed pressure (within some specified tolerance), it is desirable to choose an initial pressure that is a good estimate of the actual Hugoniot pressure. Although we will show in section 3 that the AE-EOS method is largely

Table 1. Estimates of the initial pressure for shocked liquid N_2.[a]

T/K	Mole fraction $x(N_2)$	Mole fraction $x(N)$	V/cm^3 g^{-1}	E/kJ g^{-1}	$P_{\text{initial guess}}$/GPa	[b]P_{Hg}/GPa	% difference[c]
536.2	1.0	0.0	0.866	0.09181	2.82	2.96	4.7
883.9	1.0	0.0	0.866	0.3762	4.35	4.74	8.2
2008.4	1.0	0.0	0.866	1.435	10.1	10.1	0.0
3912.4	1.0	0.0	0.866	3.385	20.6	18.1	−13.8
6778.1	1.0	0.0	0.866	6.434	37.0	29.9	−23.7
7963.0	1.0	0.0	0.866	7.745	44.0	36.0	−22.2
9557.7	1.0	0.0	0.866	9.622	54.1	47.0	−15.1
10185.4	1.0	0.0	0.866	10.41	58.4	52.6	−11.0
10935.2	1.0	0.0	0.866	11.4	63.7	60.4	−5.5
12588.9	1.0	0.0	0.866	13.8	76.4	81.1	5.8

[a]Quantities shown are based on the estimating scheme described in the text.
[b]Taken from [10].
[c]% difference $= 100 \times (P_{Hg}\text{-}P_{\text{initial guess}})/P_{H_g}$.

insensitive to the initial pressure guess, extremely poor initial guesses could result in numerical failures. For example, consider the simulation of a Hugoniot state such that $T_{H_g} > T_o$ (recall that T_{H_g} is the temperature of the chosen Hugoniot state and T_o is the temperature of the unshocked material). If the initial guess of the pressure, $P_{\text{initial guess}}$, causes an expansion of the simulation cell such that the specific volume is larger than the specific volume of the unshocked material, a negative pressure value will be predicted. From a practical standpoint, this is an unphysical occurrence since it implies that the material has expanded upon shock rather than being compressed. Furthermore, from a computational standpoint, the simulation cell will never converge to a negative imposed pressure. Such an occurrence, however, is analogous to choosing a starting configuration that relaxes to a physically unreasonable and computationally inconsistent state.

Consider the following *ad hoc* approach to choosing a reasonable initial guess of the pressure for equation (3). First, assume that the shocked material does not decompose (i.e. chemically react). This is a reasonable approximation at low shock pressures and reduces the first term on the right-hand side of equation (5) to $H^o_{\text{starting material}}$. Next, neglect the contribution of U^{conf} and thus eliminate the second term on the right-hand side of equation (5). This approximation has no physical justification, however a short simulation could be performed to calculate U^{conf} (although probably unnecessary given the lack of sensitivity of the final result on the initial guess of the pressure). Finally, estimate the amount of compression the starting material will undergo, e.g. $V = 0.7V_o$. This estimate presumably can be predicated on previous studies of the material or similar materials. With these approximations, an initial estimate of the Hugoniot pressure can be determined.

Estimates of the initial pressures for shocked liquid N_2 simulations using this scheme are compared with Hugoniot pressures calculated in an earlier study [10] in Table 1. Small differences between $P_{\text{initial guess}}$ and P_{H_g} are found at low pressures. Obvious improvements at higher pressures can be made by increasing the estimate of the amount of compression of the starting material. More importantly however, in section 3, we assess the effect of the initial guess of the pressure on the stability and accuracy of the AE-EOS method. As will be shown, the estimates in Table 1 provide more than sufficient initial guesses, since guesses as large as ±67% P_{H_g} converge properly. Furthermore, as points along the Hugoniot curve are determined, better estimates of the initial pressure can be made by using these Hugoniot states.

2.2.3. *Averaging*

For completeness of study, we consider three different schemes for averaging the instantaneous values of H_g and dH_g/dP, which are then used in equation (3): (1) *block* averages; (2) *running* averages; and (3) *block-to-running* averages. Block averages are taken from a limited number of configurations immediately preceding the pressure adjustment step, while running averages are taken continuously over all configurations generated during the simulation run. The block-to-running averages scheme uses a block-averaging scheme for the equilibration period of the simulation run and then continues with a running average scheme for the production period. This scheme may most effectively remove the effects of a poor initial guess, while we expect the running average scheme to be the most effective alternative since fluctuations in the pressure will become increasingly damped as the simulation proceeds. Block averaging methods will likely be more

slowly converging at best, and unstable at worst. Moreover, running average schemes have been the most successful scheme in the finite-difference algorithms used in the phase coexistence methods mentioned previously [43–45].

2.2.4. *Pressure prediction frequency*

We also consider the effect of the frequency of re-setting the pressure during the simulation. Less frequent updates are expected to cause the results to converge more slowly while more frequent updates could possibly cause the root-finding scheme to become unstable or to fluctuate too greatly.

A final note on the convergence of the system to the predicted pressure is considered. Step (4) in the algorithm outline (see section 2.1) allows the system to converge to the predicted pressure value (within a few % of the predicted pressure for the most recent simulation steps) before re-evaluating the Hugoniot expression and its derivative ($\mathrm{d}H_g/\mathrm{d}P$) in the equilibration period only. This ensures that even for large changes in the predicted pressure, equilibrated information is still used in the H_g and $\mathrm{d}H_g/\mathrm{d}P$ calculation. Typically, these large changes will only occur during the earliest stages of the simulation. At later times during the production cycles, this criterion is nearly always satisfied.

3. Application: shock Hugoniot states of liquid N_2

For demonstrative purposes, several shock Hugoniot states of liquid nitrogen are considered. The shock Hugoniot properties were predicted based on the initial states calculated previously: $T = 77.0\,\mathrm{K}$; $\rho = 0.808\,\mathrm{g\,cm^{-3}}$; $P = 50.49\,\mathrm{MPa}$; $E = -0.441\,\mathrm{kJ\,g^{-1}}$ [10]. At pressures higher than ~30 GPa along the Hugoniot curve, the dissociation reaction of molecular nitrogen ($N_2 \Leftrightarrow 2N$) occurs. Therefore, we demonstrate the AE-EOS method using the molecular dynamics technique only at pressures below 30 GPa while we demonstrate the AE-EOS method using the RxMC method at a wider range of pressures. Particles interact through the exponential-six potential, which can be expressed as

$$U_{\exp-6}(r) = \begin{cases} \infty, & r < r_{\mathrm{core}}, \\ \dfrac{\varepsilon}{1-(6/\alpha)}\left[\dfrac{6}{\alpha}\exp\left(\alpha\left[1-\dfrac{r}{r_{\mathrm{m}}}\right]\right)-\left(\dfrac{r_{\mathrm{m}}}{r}\right)^6\right], & r \geq r_{\mathrm{core}}, \end{cases} \tag{8}$$

where ε is the depth of the attractive well between particles, r_{m} is the radial distance at which the potential is a minimum, while α controls the steepness of the repulsive interaction. The cut-off distance r_{core} is included to avoid the unphysical singularity in the potential function as $r \to 0$. r_{core} is the smallest positive value for which $\mathrm{d}U_{\exp-6}(r)/\mathrm{d}r = 0$ and is obtained by iterative solution of equation (8). The potential parameters for the species considered in this work are given in Table 2. A spherical cut-off for the particle–particle interactions was applied at $2.5r_{\mathrm{m,N_2}}$ with long-range corrections added to account for interactions beyond this distance [48]. Electrostatic interactions between species were ignored. The unlike interactions between species i and j were approximated by the Lorentz–Berthelot combining rules [49] for ε_{ij}, α_{ij} and $r_{\mathrm{m},ij}$:

Table 2. Exponential-6 potential parameters [47].

Species	r_{core}/Å	r_m/Å	$\varepsilon/k_b k^{-1}$	α
N_2	1.13	4.2005	101.10	12.684
N	0.98	2.5688	88.181	11.013

$$\varepsilon_{ij} = (\varepsilon_i\varepsilon_j)^{1/2}; \quad \alpha_{ij} = (\alpha_i\alpha_j)^{1/2}; \quad r_{\mathrm{m},ij} = (r_{\mathrm{m},i} + r_{\mathrm{m},j})/2\,; \tag{9}$$

while

$$r_{\mathrm{core},ij} = (r_{\mathrm{core},i} + r_{\mathrm{core},j})/2. \tag{10}$$

3375 N_2 molecules were used with all calculated quantities reduced by the exponential-6 potential energy (ε) and size (r_{m}) parameters of N_2. Periodic boundary conditions were imposed for all dimensions. Thermochemical reference data were used in calculating the ideal-gas enthalpies (H_i^{o}) required in equation (5) [50, 51].

3.1. *Molecular dynamics*

3.1.1. *Simulation details*

Molecular dynamics simulations in the isothermal–isobaric ensemble were performed using the leap-frog Verlet algorithm [46, 48] and the Melchionna modification of the Hoover–Nosé equations of motion [52]. A thermostatting rate of $50\,\mathrm{ps^{-1}}$ was used to maintain the imposed temperature while a barostatting rate ranging from 0.032–0.042 $\mathrm{ps^{-1}}$ was used to maintain the imposed pressure. Initial configurations were generated from a face-centred-cubic (fcc) lattice structure with initial particle velocities selected from a Boltzmann distribution that corresponded to the imposed temperature. Preceded by an equilibration period of 0.127–0.254 ns during which the pressure was not re-set using equation (3), trajectories were followed for 1.32 ns with time steps ranging from 0.00763–0.0102 ps. All pressure values reported were determined using the virial theorem [46].

3.1.2. *AE-EOS method details*

Three state points along the shock Hugoniot curve were determined: $T = 883.9$; 3912.4; 6778.1 K. These state points are below the regime in which N_2 dissociates into atomic nitrogen. For each point, the Hugoniot pressure (P_{H_g}) was predicted in two simulations, one in which the initial pressure was much lower than the Hugoniot pressure and one in which the initial pressure was too high. The values of the initial guesses are given in Table 3 and correspond to differences in the known value [10] by ±67%. The effect of the frequency of re-setting the imposed pressure was also studied. Two cases were considered, re-setting at: (a) every 100 steps; and (b) every 500 steps. Following the initial equilibration period used to relax the system from the fcc crystal to the imposed thermodynamic condition, an additional 0.305 ns of the trajectory was used to further equilibrate the system after the AE-EOS algorithm is implemented (i.e. the pressure is re-set at specified intervals). All quantities calculated during this time interval were not included in the final averages. A tolerance value of ±5% was used in Step (4) for the pressure (see section 2.1), i.e. the calculated pressure was required to be within ±5% of the most recent P_{H_g} prediction before re-evaluating H_g and dH_g/dP and re-setting of the imposed pressure.

3.1.3. *Results*

A comparison between the Hugoniot properties predicted using the original E-EOS and AE-EOS methods is shown in table 3. Good agreement is found for all cases considered, with pressure and specific volume values well within statistical uncertainty. Figures 1 (*a*) and (*b*) are the instantaneous values every 100th time-step for the Hugoniot expression (equation (5)) and the predicted pressure (equation (3)), respectively, at the Hugoniot point $T = 883.9$ K. The results converge within a few thousand time-steps. The figures show that H_g fluctuates about zero and the predicted pressures converge to P_{H_g}.

Table 3 also shows that no dependence on the initial pressure guess is found, with values within a few percent of the E-EOS method results. A graphical demonstration of the stability of the algorithm is given in Figures 1 (*c*) and (*d*) for the $T = 6778.1$ K point along the H_g curve. In figure 1 (*c*) the fluctuations of the H_g expression are shown to increase sporadically throughout the simulation but the scheme 'recovers' within a few thousand time-steps. A plot of the predicted pressure for this point (figure 1 (*d*)) shows that the pressure predicted in the Newton–Raphson scheme remains stable during these occasional fluctuations of the H_g value.

As expected, fluctuations are more balanced when the H_g expression is evaluated less frequently since the system configuration is allowed longer to converge to the predicted pressure. This is evident by comparing figures 1 (*c*) and (*e*), where the difference between the data shown is based on the frequency of the H_g evaluation and imposed pressure re-set: figure 1 (*c*) is for every 100 time-steps, while figure 1 (*e*) is for every 500 time-steps. While fluctuations may be steadier for less frequent evaluations, still no noticeable dependencies of the final values of P_{H_g} and V_{H_g} on the frequency

Table 3. Predicted shock Hugoniot states of liquid N_2 using molecular dynamics in the AE-EOS method.[a]

	H_g evaluation frequency							
	Every 100 steps				Every 500 steps			
$P_{initial}$/GPa	T/K	P/GPa	V/cm^3/mol N_2	H_g/kJ g^{-1}	T /K	P/GPa	V /cm^3 mol^{-1} N_2	H_g/kJ g^{-1}
[b]$T = 883.9$ K ; $P = 4.74$ GPa $V = 19.82$ cm^3 mole^{-1} N_2								
1.56	883.9 (1.2)	4.82 (9)	19.7 (2)	−2.356E-4 (0.013)	883.9 (1.1)	4.8 (1)	19.9 (3)	8.901E-3 (0.16)
7.92	883.9 (1.2)	4.81 (2)	19.74 (3)	1.001E-4 (0.023)	883.9 (1.2)	4.8 (1)	20.0 (3)	1.600E-2 (0.19)
[b]$T = 3912.4$ K ; $P = 18.1$ GPa $V = 15.57$ cm^3 mole^{-1} N_2								
5.97	3912 (52)	18.4 (3)	15.6 (2)	−1.550E-3 (0.15)	3912 (52)	18.4 (2)	15.6 (2)	−3.101E-5 (0.043)
30.23	3912 (53)	18.4 (1)	15.56 (8)	2.790E-3 (0.063)	3912 (54)	17.8 (6)	16.0 (4)	1.841E-1 (1.1)
[b]$T = 6778.1$ K ; $P = 29.9$ GPa $V = 14.05$ cm^3 mole^{-1} N_2								
9.87	6778 (94)	29.9 (4)	14.1 (2)	−1.867E-3 (0.25)	6778 (94)	29.9 (9)	14.1 (4)	1.511E-1 (1.6)
49.93	6778 (93)	29.9 (5)	14.1 (2)	−5.581E-3 (0.35)	6778 (94)	29.9 (5)	14.1 (2)	1.355E-4 (0.13)

[a]Quantities are ensemble averages. Uncertainties in units of the last decimal digit are given in parentheses: *e.g.*, 883.9 (1.2) means 883.9 ± 1.2, except for the uncertainties of H_g where the values given in parentheses are absolute values. Uncertainties reported were determined from the standard deviation of the instantaneous values.

[b]Hugoniot states taken from [10].

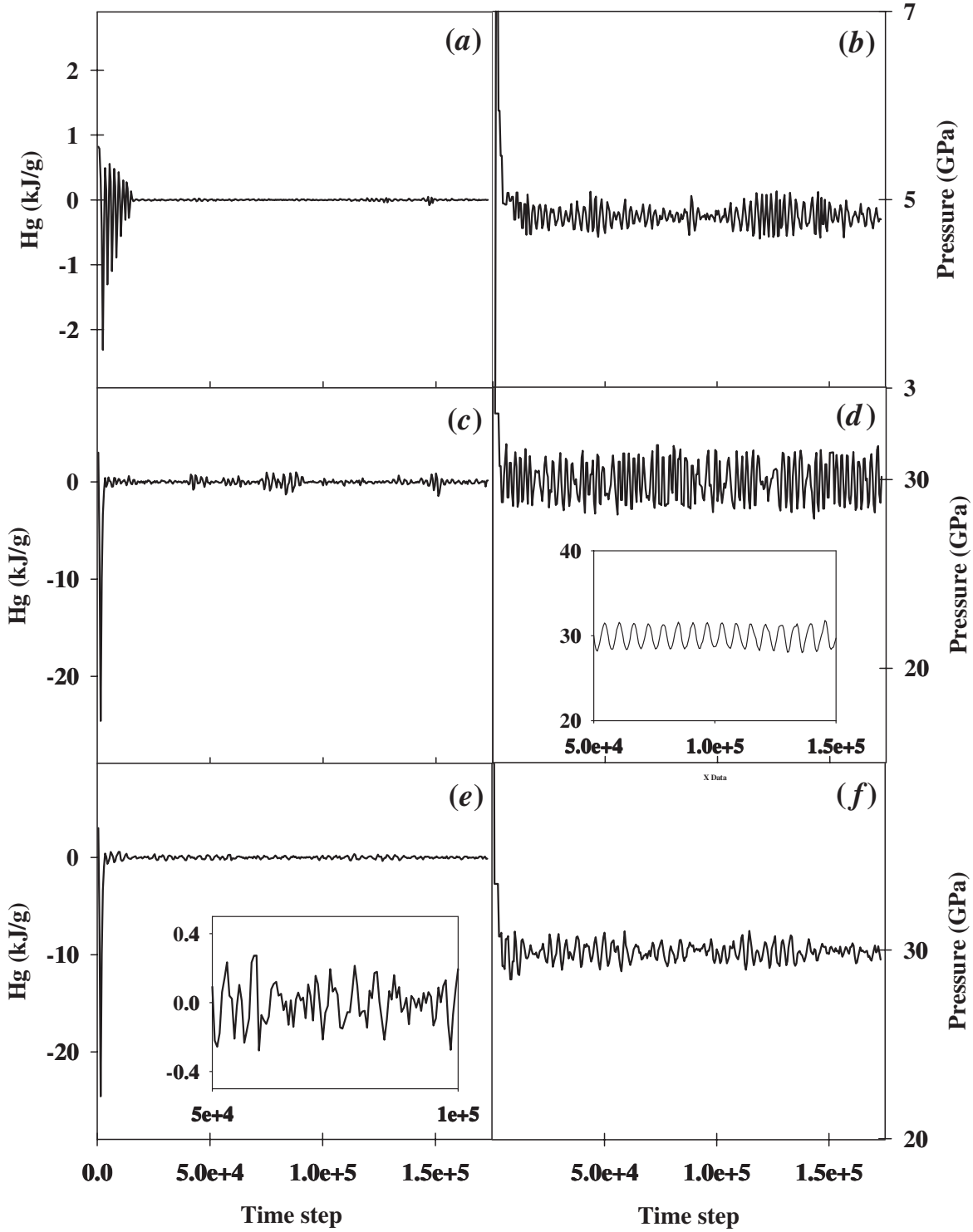

Figure 1. Instantaneous simulation results for predicted points along the Hugoniot curve: (*a*)–(*b*) $T = 883.9$ K point with a frequency of H_g evaluation and subsequent pressure re-set every 100 time steps and initial pressure guess of 1.56 GPa; (*c*)–(*d*) $T = 6778.1$ K point with a frequency of H_g evaluation and subsequent pressure re-set every 100 time steps and initial pressure guess of 49.93 GPa; (*e*)–(*f*) same as (*c*)–(*d*), except the frequency of H_g evaluation and subsequent pressure re-set is every 500 time steps. The left-most frame of each set shows the value of the Hugoniot expression calculated from equation (5) and the right-most frame is the pressure predicted by equation (3). Inset in (*e*) shows fluctuations of H_g while the inset in (*d*) shows the fluctuations in the pressure for an isothermal–isobaric ensemble molecular dynamics simulation carried out at $P = 29.9$ GPa and $T = 6778.1$ K.

of the H_g evaluation and subsequent re-setting of the pressure are found. For comparison, the inset in figure 1 (*d*) shows the fluctuations in the calculated pressure for an isothermal–isobaric ensemble molecular dynamics simulation carried out at $P = 29.9$ GPa and $T = 6778.1$ K.

3.2. *Reactive Monte Carlo*

3.2.1. *Simulation details*

The reactive Monte Carlo method was used to assess the accuracy of the AE-EOS method at a wider range of conditions than considered using the molecular dynamics technique including conditions under which N_2 dissociates ($N_2 \Leftrightarrow 2N$). Details of the methodology can be found in the original papers [53–55] as well as in recent applications of the technique, which implemented the E-EOS method [10]. In addition to intermolecular potentials that describe non-reactive interactions between species N_2 and N in the equilibrium mixture, RxMC also requires inputting the ideal-gas internal modes (vibration, rotation, electronic). The vibrational and rotational contributions to the ideal-gas partition functions of both species were calculated using a standard source [56], and supplemented with electronic level constants that included the ground state and six excited electronic states for N_2 [50], along with electronic energy levels for N taken from Moore and Gallagher [51].

Constant-pressure RxMC simulations of shocked N_2 were initiated from 3375 N_2 particles placed on an fcc lattice structure. Simulations were performed in steps, where a step (chosen with equal probability) was either a particle displacement, a forward reaction step, or a reverse reaction step. A change in the simulation cell volume was attempted every 500 steps. Simulations were equilibrated for 1.5×10^6 steps after which averages of the quantities were taken over 8×10^6 steps. Uncertainties were estimated using the method of block averages by dividing the production run into 10 equal blocks [48]. Reported uncertainties are one standard deviation of the block averages. (Note that these block averages do not correspond to the averaging used in the P_{H_g} prediction scheme.) The maximum displacement and volume change were adjusted to achieve an acceptance fraction of approximately 0.33 and 0.5, respectively. Depending on the system conditions, the acceptance fraction of the reaction steps ranged from 0.075–0.375.

3.2.2. *AE-EOS method details*

Three points along the shock Hugoniot curve were considered: $T = 2008.4$; 7963.03; 10935.2 K. Again for each point, P_{H_g} was predicted from two initial guesses (values are given in Tables 4–6) that differ from the known value [10] by ±67%. We predicted the shock Hugoniot properties based on the same initial state used previously [10] and in the molecular dynamics study above. A tolerance value of ±2.5% was used in Step 4 for the pressure (see section 2.1), a value slightly lower than used in the molecular dynamics simulations above. Analogous to the study above, the effect of the frequency of re-evaluating the Hugoniot pressure and subsequent re-setting of the imposed pressure was studied. Two cases were considered, re-setting at: (a) every 5000 steps; and (b) every 50 000 steps. Additionally, three different averaging schemes of the instantaneous values of H_g and dH_g/dP were assessed: (a) block averages; (b) running averages; and (c) block-to-running averages. A description of each type is given in section 2.2. For each of the initial pressure guesses, all six series (2 H_g frequency evaluations × 3 averaging schemes) were considered.

3.2.3. *Results*

Comparisons between the Hugoniot properties predicted by the E-EOS and the AE-EOS methods are given in Tables 4–6. We find excellent agreement between the E-EOS and the AE-EOS results for all quantities calculated. Nearly all AE-EOS quantities fall within ±0.5% of the E-EOS calculations with none greater than ±0.9%. Consequently, no dependence on the initial pressure guess or the Hugoniot expression evaluation frequency is evident. Likewise, no apparent dependence on each of the averaging schemes is found. A detailed examination of the instantaneous values reveals the behaviour of the averaging schemes. Figure 2 shows the instantaneous values of the Hugoniot expression throughout the simulation run for the $T = 2008.4$ K point using an initial pressure guess of 16.9 GPa. Note that to discern the data more clearly, the 'running' and 'block-to-running' curves are offset on the *y* axis by 0.05 and 0.1 kJ g^{-1}, respectively. Updates of the imposed pressure every 50 000 steps (figure 2 (*a*)) and every 5000 steps (figure 2 (*b*)) are shown. Figures 2 (*a*) and (*b*) exhibit similar behaviour with the expected increased statistical 'noise' for figure 2 (*b*). The block-averaging scheme fluctuates throughout the simulation runs but in a consistent and stable fashion while the running-average scheme fluctuates minimally. The block-to-running averaging scheme exhibits a combination of these behaviours, balanced and steady fluctuation during the block-averaging portion followed by limited fluctuation during the running portion. Insets in figures 2 (*a*) and (*b*) show fluctuations for the running average scheme on a reduced scale. Similar fluctuations are found for the 'running' portion of the block-to-running average scheme. Other series points exhibit

Table 4. Predicted shock Hugoniot states of liquid N_2 at $T = 2008.4$ K using the reactive Monte Carlo method. Values determined previously [10] by the E-EOS method are $P = 10.1$ GPa ; $V = 17.41\,cm^3\,mole^{-1}\,N_2$; x $(N_2) = 1.00$.[a]

	H_g evaluation frequency							
	Every 5000 steps				Every 50 000 steps			
$P_{initial}$/GPa	P/GPa	V/ $cm^3\,mol^{-1}\,N_2$	[b]x (N_2)	H_g/kJ g^{-1}	P/GPa	V/ $cm^3\,mol^{-1}\,N_2$	x (N_2)	H_g/kJ g^{-1}
Block averages								
3.3	10.1 (1)	17.35 (3)	1.00 (0)	2.177E-5 (0.013)	10.1 (1)	17.35 (6)	1.00 (0)	−4.706E-6 (0.16)
16.9	10.1 (1)	17.35 (5)	1.00 (0)	−9.019E-7 (0.023)	10.1 (1)	17.35 (4)	1.00 (0)	−2.479E-5 (0.19)
Running averages								
3.3	10.1 (1)	17.32 (1)	1.00 (0)	−2.716E-5 (0.15)	10.2 (1)	17.33 (10)	1.00 (0)	−1.357E-4 (0.043)
16.9	10.2 (1)	17.32 (13)	1.00 (0)	−2.549E-5 (0.063)	10.2 (1)	17.33 (9)	1.00 (0)	−1.648E-4 (1.1)
Block → Running averages								
3.3	10.1 (1)	17.35 (9)	1.00 (0)	8.119E-6 (0.25)	10.1 (1)	17.34 (11)	1.00 (0)	1.816E-5 (1.6)
16.9	10.1 (1)	17.35 (8)	1.00 (0)	−4.286E-6 (0.35)	10.1 (1)	17.35 (7)	1.00 (0)	−1.508E-5 (0.13)

[a]Quantities are ensemble averages. Reported uncertainties shown in parentheses are one standard deviation of the block averages [48] and are given in units of the last decimal digit, *e.g.*, 17.35 (3) means 17.35 ± 0.03.

[b]Mole fraction of N_2, so $x(N_2) = N_{N_2}/N_{total}$ and $x(N) = 1/2N_N/N_{total}$, where $N_{total} = 3375$.

Table 5. Predicted shock Hugoniot states of liquid N_2 at $T = 7963.0$ K using the reactive Monte Carlo method. Values determined previously [10] by the E-EOS method are $P = 36.0$ GPa ; $V = 13.35\,cm^3\,mole^{-1}\,N_2$; $x\,(N_2) = 0.975$.[a]

	H_g evaluation frequency							
	Every 5000 steps				Every 50 000 steps			
$P_{initial}$/GPa	P/GPa	V/ $cm^3\,mol^{-1}\,N_2$	x (N_2)	H_g/kJ g^{-1}	P/GPa	V/ $cm^3\,mol^{-1}\,N_2$	x (N_2)	H_g/kJ g^{-1}
Block averages								
11.9	36.1 (1)	13.33 (6)	0.975 (1)	2.129E-5 (0.013)	36.2 (1)	13.32 (3)	0.975 (1)	−5.957E-4 (0.16)
60.1	36.1 (1)	13.33 (6)	0.975 (1)	1.118E-4 (0.023)	36.1 (1)	13.33 (4)	0.975 (1)	2.937E-5 (0.19)
Running averages								
11.9	36.2 (1)	13.32 (8)	0.975 (1)	−2.435E-5 (0.15)	36.1 (1)	13.33 (6)	0.975 (1)	5.444E-6 (0.043)
60.1	36.2 (1)	13.32 (6)	0.975 (1)	−1.022E-5 (0.063)	36.1 (1)	13.33 (6)	0.975 (1)	−2.631E-5 (1.1)
Block → Running averages								
11.9	36.1 (1)	13.33 (4)	0.975 (1)	1.942E-5 (0.25)	36.1 (1)	13.33 (4)	0.975 (1)	−6.005E-4 (1.6)
60.1	36.1 (1)	13.33 (2)	0.975 (1)	2.088E-5 (0.35)	36.1 (1)	13.33 (4)	0.975 (1)	−1.805E-4 (0.13)

[a]See table 4 for details.

similar behaviour, though again with no particular averaging scheme demonstrating noticeable results. This behaviour gives testament to the AE-EOS method's overall stability and robustness.

4. Discussion

We have presented a computationally efficient methodology for calculating the shock Hugoniot properties of materials using classical molecular simulations. The method is an extension of the Erpenbeck EOS approach and allows for the determination of a point along the Hugoniot curve from a single simulation. The method, termed the adaptive Erpenbeck equation of state method (AE-EOS), uses a numerical estimate of the root of the Hugoniot expression to determine the corresponding thermodynamic state. AE-EOS is applicable for any simulation method that determines points along the Hugoniot curve by generating EOS points, which includes molecular dynamics [46, 48], reactive Monte Carlo [53, 54] and the composite Monte Carlo method [11]. The method was demonstrated to be accurate and numerically stable. For the systems in this study, the method was not particularly sensitive

Table 6. Predicted shock Hugoniot states of liquid N_2 at $T = 10935.2$ K using the reactive Monte Carlo method. Values determined previously [10] by the E-EOS method are $P = 60.4$ GPa ; $V = 10.97\,cm^3\,mole^{-1}$ N_2; $x(N_2) = 0.821$.[a]

	H_g evaluation frequency							
	Every 5000 steps				Every 50 000 steps			
$P_{initial}$/GPa	P/GPa	V/ cm^3/mol^{-1} N_2	x (N_2)	H_g/kJ g^{-1}	P/GPa	V/ $cm^3\,mol^{-1}$ N_2	x (N_2)	H_g/kJ g^{-1}
Block averages								
20.0	60.6 (1)	10.95 (9)	0.820 (2)	9.934E-5 (0.013)	60.7 (1)	10.95 (9)	0.820 (2)	2.759E-3 (0.16)
100.9	60.6 (1)	10.95 (1)	0.820 (3)	2.528E-5 (0.023)	60.6 (1)	10.96 (8)	0.820 (1)	−8.182E-4 (0.19)
Running averages								
20.0	60.7 (1)	10.95 (6)	0.820 (2)	−5.219E-5 (0.15)	60.6 (1)	10.95 (4)	0.819 (1)	−4.466E-5 (0.043)
100.9	60.7 (1)	10.95 (3)	0.820 (1)	−3.152E-5 (0.063)	60.7 (1)	10.94 (5)	0.820 (2)	−4.217E-4 (1.1)
Block → Running averages								
20.0	60.5 (1)	10.96 (6)	0.820 (1)	2.017E-5 (0.25)	60.6 (1)	10.96 (7)	0.820 (2)	1.909E-3 (1.6)
100.9	60.7 (1)	10.95 (7)	0.820 (2)	−1.463E-4 (0.35)	60.6 (1)	10.95 (3)	0.820 (1)	2.541E-4 (0.13)

[a]See table 4 for details.

to the algorithm parameters, indicating the method's robustness and ability to be readily implemented. Furthermore, substantial savings in the computational requirements are gained through the implementation of the AE-EOS method. For comparable statistical uncertainty, four to five complete simulations are required to generate a single point on the Hugoniot curve for the original Erpenbeck method, while only a single simulation is needed in the AE-EOS method. Hence, a computational gain of approximately four–five-fold is made when implementing the AE-EOS method. Overall, the AE-EOS method appears to be slightly more accurate and stable when applied to the RxMC method as compared to the molecular dynamics method. This may be attributed to the relative stability of the Monte Carlo method over the molecular dynamics technique for constant-temperature and constant-pressure simulations.

The AE-EOS method is intended as an alternative tool to similar techniques, namely piston-driven molecular dynamics [7, 8] and uniaxial Hugoniostat molecular dynamics [9], since AE-EOS offers some notable advantages when simulating reactive mixtures. The most striking advantage is that the AE-EOS method does not require either: (1) *a priori* knowledge of the relative concentrations of each chemical species in the shocked state; or (2) a reactive potential that simulates bond breaking and bond formation. At least one of these conditions must be met for the other methods to be applicable to the simulation of reactive mixtures.

Extensions as well as different adaptations of the AE-EOS method are possible. For example, as outlined in section 2.1, there exist several choices of independent variables that the ensemble can be based upon (these choices are considered in the Appendix). Furthermore, as discussed in section 2.2 other numerical root-finding algorithms that converge the simulation to $H_g = 0$ are possible. Simplicity and generality in implementing the method, however, has led to the choices presented here. Besides the numerical-based approaches described in this work, other approaches based on the modification or invention of a statistical ensemble may be possible. For example, through the development of an NVE-RxMC ensemble, where $E = E_o + \frac{1}{2}(P + P_o)(V_o - V)$; N and V are held constant, while E will fluctuate (the kinetic energy will be kept nearly constant). In addition to the standard RxMC moves, attempts to randomly change E will be made with the acceptance of the move based on

$$P \propto \begin{cases} \dfrac{\varepsilon}{\varepsilon^2 - H_g}, & \text{for } |H_g| < \Delta, \\ 0, & \end{cases} \tag{11}$$

where ε is an arbitrary parameter defining the width of the Δ function. The method would be similar to NVE-MC [46] but with the additional RxMC-type reaction moves. A still more rigorous and fundamental approach is the development of a constant-H_g ensemble, i.e. the development of an NVH_g-RxMC, NPH_g-RxMC, or NTH_g-RxMC ensemble. RxMC moves would be accepted based on criteria derived specific to these ensembles. Although in principle it may be possible to determine an expression for the partition functions for such ensembles, it may not be possible to derive expressions with a practical form (e.g. which neatly separate inter- and intramolecular terms). If such a method is plausible, it would be analogous to the

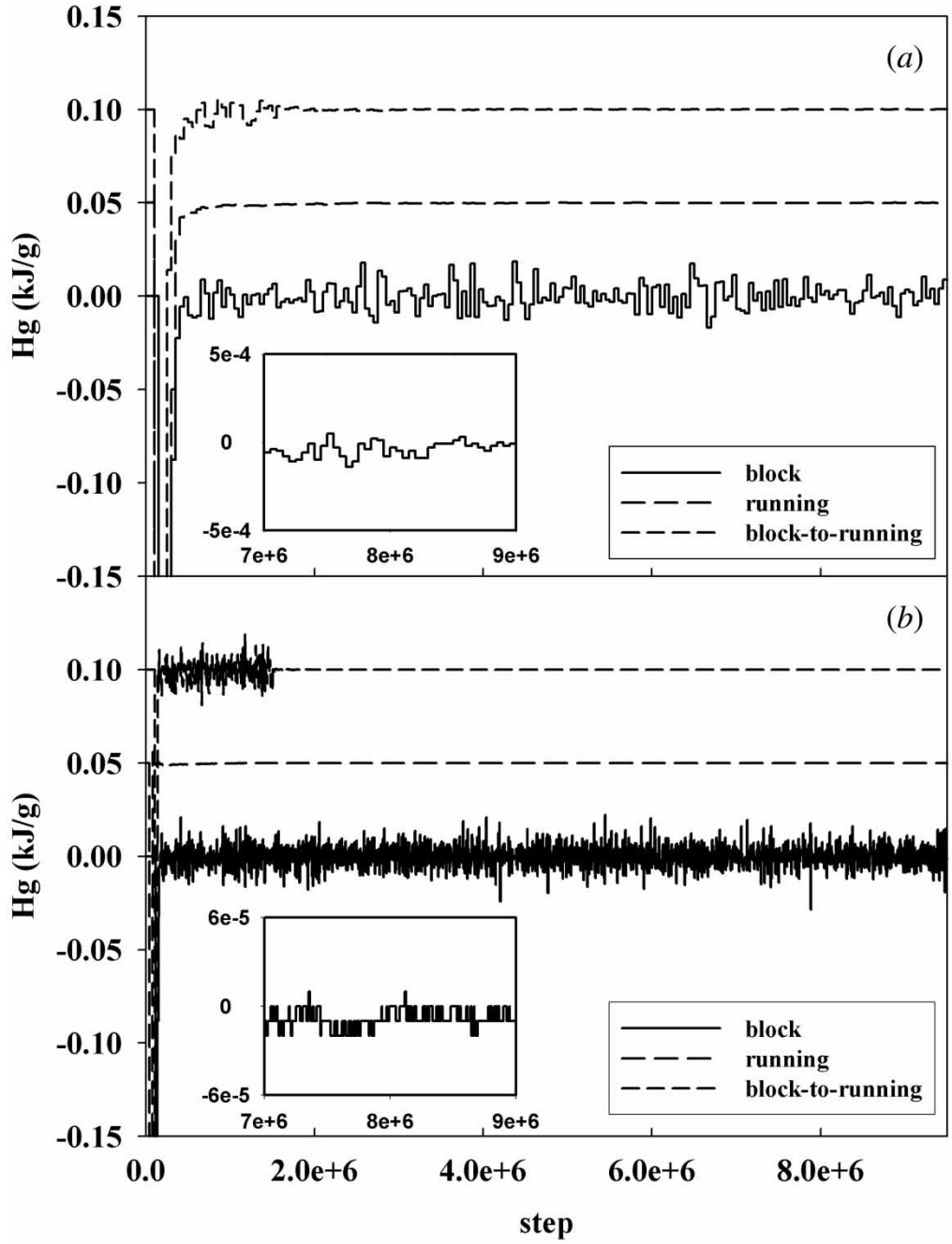

Figure 2. Instantaneous values of the Hugoniot expression for the $T = 2008.4$ K point using the reactive Monte Carlo method where the initial pressure guess is 16.9 GPa. Frequency of H_g evaluation is shown for: (*a*) every 50 000 steps; and (*b*) every 5000 steps. Curves corresponding to 'running' and 'block-to-running' notation in the legend have been shifted by 0.05 and 0.1 kJ g^{-1}, respectively.

uniaxial Hugoniostat-MD method. It remains to be seen, however, if such methods would offer any computational advantage over the current methods.

The authors are grateful to Martin Lísal (Czech Academy of Sciences) for helpful discussions and critical reading of part of this manuscript. This work was performed while JKB held a National Research Council Research Associateship Award at the US Army Research Laboratory. The calculations reported in this work were performed at the U.S. Army Research Laboratory Major Shared Resource Center, Aberdeen Proving Ground, MD. The software used in the molecular dynamics simulations was developed under the DOD High Performance Computing Software Support Initiative (CHSSI) for Computational Chemistry and Material Science (CCM-5).

Appendix

In section 2.1 we derived the AE-EOS method for pressure as the independent variable in the root-finding algorithm. Let us consider the other possible choices of the independent variable when implementing this approach, namely, E, T and V. The choice of any of these variables requires an ensemble for which this particular variable is fixed. Therefore, when $x_n = E$, a constant-E ensemble is required. The original molecular dynamics technique is based upon such an ensemble (NVE) [46]. Furthermore, a direct Monte Carlo method for atomic models in an NVE ensemble has been developed [57, 58] and was recently extended to molecular models that include all internal modes in the internal energy [59]. However, the choice of constraining E is somewhat less convenient when calculating points along the Hugoniot, since typically experimental measurements provide P–V/V_o or P–T curves.

The choice of $x_n = V$ can be eliminated due to the possibility of encountering spurious circumstances during a molecular simulation. For example, for each iteration of the root-finding algorithm a new simulation cell volume will be predicted. However, a change in the simulation cell volume during a molecular simulation typically requires a rescaling of the particle positions (techniques exist which avoid total particle rescaling but apply to less general cases). Therefore, in cases where the predicted volume is considerably smaller than the current volume (which may occur during the first step when a poor initial guess of the Hugoniot volume is made) it is likely that a significant number of particles will have substantial overlap and create an energetically unfavourable configuration. For Monte Carlo simulations, this is less prohibitive but for molecular dynamics simulations such a situation could cause significant deviations in the conservation of energy and momentum constraints. For this reason V as the independent variable in the AE-EOS method may not be appropriate.

Finally for $x_n = T$, consider the derivative term required in equation (2)

$$\begin{aligned} f'(x_n) &= \frac{\mathrm{d}H_\mathrm{g}}{\mathrm{d}T} \\ &= \frac{\mathrm{d}}{\mathrm{d}T}\left(\sum_{i=1}^{c_j} y_i H_i^\mathrm{o}\right) + \frac{\mathrm{d}}{\mathrm{d}T}\left(U^\mathrm{conf}\right) - \frac{\mathrm{d}}{\mathrm{d}T}(RT) \\ &\quad - \frac{1}{2}\frac{\mathrm{d}}{\mathrm{d}T}(PV_0 - PV + P_0V_0 - VP_0). \end{aligned} \tag{A1}$$

Note that analogous to the derivation of equation (7), we consider the quantities in this expression to be instantaneous values that depend only on the current configuration. The first term on the right-hand side of equation (A1) can usually be analytically determined since H_i^0 can be written as a function of T (and often is determined from the heat capacity, C_p, in this form). The second term on the right-hand side is eliminated from equation (A1) since $U^\mathrm{conf} = U^\mathrm{conf}(r)$ only, while the third term reduces to R. The last term can be expanded so that

$$\begin{aligned} &\frac{1}{2}\frac{\mathrm{d}}{\mathrm{d}T}(PV_0 - PV + P_0V_0 - VP_0) \\ &\quad = -\frac{1}{2}\left[\frac{\mathrm{d}}{\mathrm{d}T}(PV_0) - \frac{\mathrm{d}}{\mathrm{d}T}(PV) + \frac{\mathrm{d}}{\mathrm{d}T}(P_0V_0) - \frac{\mathrm{d}}{\mathrm{d}T}(VP_0)\right]. \end{aligned} \tag{A2}$$

Simplifying equation (A2), we see that the first two terms on the right-hand side require further evaluation of a $\mathrm{d}P/\mathrm{d}T$ term, while the third term is eliminated since P_0 and V_0 are constant. If we consider the standard virial equation typically used in molecular simulation to calculate an instantaneous pressure (see e.g. [46]), then

$$P = P_{\substack{\mathrm{ideal}\\ \mathrm{gas}}} + P_\mathrm{excess} = \rho kT - \frac{1}{3}\sum_i \sum_{j>i} r\frac{\mathrm{d}U^\mathrm{conf}}{\mathrm{d}r}, \tag{A3}$$

where the summations are taken over all i–j particle pairs. Calculating the derivative of equation (A3) with respect to T we get $\mathrm{d}P/\mathrm{d}T = \rho k$ since

$$U^\mathrm{conf} \neq U^\mathrm{conf}(T). \tag{A4}$$

Finally, however the second and fourth terms of equation (A2) require a $\mathrm{d}V/\mathrm{d}T$ term. From the simulation, we have no means of evaluating this term and *a priori* knowledge of $V = V(T)$ is unlikely. A functional fit of $V = V(T)$ could be determined as the simulation proceeds but would be counter-productive to our overall goal of determining a Hugoniot state from a single simulation of reasonable length. The choice of $x_n = T$ in equation (2) therefore seems less practical.

References

[1] Touret, J., and van den Kerkhof, A. M., 1986, *Physica* B & C, **139,** 834.
[2] Kortbeek, P. J., Seldam, C. A. T., and Schouten, J. A., 1990, *Molec. Phys.*, **69,** 1001.
[3] Duan, Z., Moller, N., and Weare, J. H., 1996, *Geochim. Cosmochim. Acta*, **60,** 1209.
[4] Fickett, W., and Davis, W. C., 1979, Detonation (Berkeley: University of California Press).
[5] Ree, F. H., 1984, *J. chem. Phys.*, **81,** 1251.
[6] Fried, L. E., 2001, Cheetah 3.0 User's Manual, (manuscript number UCRL-MA-117541, Revision 3) (Livermore, CA: Lawrence Livermore National Laboratory).
[7] Swanson, D. R., Mintmire, J. W., Robertson, D. H., and White, C. T., 2000, *Chem. Phys. Reps.*, **18,** 1871.

[8] Robertson, D. H., Brenner, D. W., and White, C. T., 1991, *Phys. Rev. Lett.*, **67,** 3132.
[9] Maillet, J. B., Mareschal, M., Soulard, L., Ravelo, R., Lomdahl, P. S., Germann, T. C., and Holian, B. L., 2000, *Phys. Rev.* E, **63,** 016121.
[10] Brennan, J. K., and Rice, B. M., 2002, *Phys. Rev.* E, **66,** 021105.
[11] Shaw, M. S., 2002, 12th Detonation Symposium, San Diego, 11–16 August; 2001, *Shock Compression of Condensed Matter*, *AIP Conference Proceedings*, Atlanta, 24–29 June, edited by M. D. Furnish, N. N. Thadhani and Y. Horie (Melville, NY: AIP).
[12] Erpenbeck, J. J., 1992, *Phys. Rev.* A, **46,** 6406.
[13] Rice, B. M., Mattson, W., Grosh, J., and Trevino, S. F., 1996, *Phys. Rev.* E, **53,** 611.
[14] Karo, A. M., Hardy, J. R., and Walker, F. E., 1978, *Acta Astronaut.*, **5,** 1041.
[15] Powell, J. D., and Batteh, J. H., 1978, *J. appl. Phys.*, **49,** 3933.
[16] Powell, J. D., and Batteh, J. H., 1979, *Phys. Rev.* B, **20,** 1398.
[17] Powell, J. D., and Batteh, J. H., 1980, *J. appl. Phys.*, **51,** 2050.
[18] Holihan, B. L., Hoover, W. G., Moran, B., and Straub, G. K., 1980, *Phys. Rev.* A, **22,** 2798.
[19] Tsai, D. H., and Trevino, S. F., 1984, *J. chem. Phys.*, **81,** 5636.
[20] Tsai, D. H., 1990, Chemistry and Physics of Energetic Materials, edited by S. N. Bulusu (Dordrecht: Kluwer).
[21] Brenner, D. W., 1992, Shock Compression of Condensed Matter (Amsterdam: Elsevier).
[22] Robertson, D. H., Brenner, D. W., Elert, M. L., and White, C. T., 1992, Shock Compression of Condensed Matter (Amsterdam: Elsevier).
[23] White, C. T., Robertson, D. H., Elert, M. L., and Brenner, D. W., 1992, Microscopic Simulations of Complex Hydrodynamic Phenomena (New York: Plenum).
[24] Brenner, D. W., Robertson, D. H., Elert, M. L., and White, C. T., 1993, *Phys. Rev. Lett.*, **70,** 2174.
[25] White, C. T., Sinnott, S. B., Mintmire, J. W., Brenner, D. W., and Robertson, D. H., 1994, *Int. J. quantum Chem. Symp.*, **28,** 129.
[26] Rice, B. M., Mattson, W., Grosh, J., and Trevino, S. F., 1996, *Phys. Rev.* E, **53,** 623.
[27] Alper, H. E., Abu-Awwad, F., and Politzer, P., 1999, *J. phys. Chem.* B, **103,** 9738.
[28] Bedrov, D., Smith, G. D., and Sewell, T. D., 2000, *J. chem. Phys.*, **112,** 7203.
[29] Bedrov, D., Smith, G. D., and Sewell, T. D., 2000, *Chem. Phys. Lett.*, **324,** 64.
[30] Bedrov, D., Ayyagari, C., Smith, G. D., Sewell, T. D., Menifoff, R., and Zaug, J. M., 2001, *J. comput.-aided mat. Design*, **8,** 77.
[31] Bunte, S. W., and Sun, H., 2000, *J. phys. Chem.* B, **104,** 2477.
[32] Bunte, S. W., and Miller, M. S., 2001, Army Research Laboratory Technical Report, ARL-TR-2496 (Aberdeen Proving Ground, MD: US Army).
[33] Smith, G. D., and Bharadwaj, R. K., 1999, *J. phys. Chem.* B, **103,** 3570.
[34] Sorescu, D. C., Rice, B. M., and Thompson, D. L., 1997, *J. phys. Chem.* B, **101,** 798.
[35] Sorescu, D. C., Rice, B. M., and Thompson, D. L., 1998, *J. phys. Chem.* A, **102,** 8386.
[36] Sorescu, D. C., Rice, B. M., and Thompson, D. L., 1998, *J. phys. Chem.* A, **102,** 8386.
[37] Sorescu, D. C., Rice, B. M., and Thompson, D. L., 1999, *J. phys. Chem.* A, **103,** 989.
[38] Sorescu, D. C., and Thompson, D. L., 1999, *J. phys. Chem.* B, **103,** 6774.
[39] Sorescu, D. C., Rice, B. M., and Thompson, D. L., 1999, *J. phys. Chem.* B, **103,** 6783
[40] Sorescu, D. C., Rice, B. M., and Thompson, D. L., 2000, *J. phys. Chem.* B, **104,** 8406.
[41] Sorescu, D. C., Boatz, J. A., and Thompson, D. L., 2001, *J. phys. Chem.* A, **105,** 5010.
[42] Weisstein, E. W., *Eric Weisstein's World of Mathematics* (*http://mathworld.wolfram.com/Root-FindingAlgorithm.html*).
[43] Kofke, D. A., 1993, *Molec. Phys.*, **78,** 1331.
[44] Kofke, D. A., 1993, *J. chem. Phys.*, **98,** 4149.
[45] Mehta, M., and Kofke, D. A., 1994, *Chem. Eng. Sci.*, **49,** 2633.
[46] Allen, M. P., and Tildesley, D. J., 1987, *Computer Simulation of Liquids* (Oxford: Oxford University Press).
[47] Fried, L. E., and Howard, W. M., 1998, *J. chem. Phys.*, **109,** 7338.
[48] Frenkel, D., and Smit, B., 2002, *Understanding Molecular Simulation* (San Diego: Academic Press).
[49] Reed, T. M., and Gubbins, K. E., 1973, Applied Statistical Mechanics (New York: McGraw-Hill).
[50] Lofthus, A., and Krupenie, P. H., 1977, *J. phys. Chem. ref. Data*, **6,** 113.
[51] Moore, C. E., and Gallagher, J. W., 1993, *Tables of Spectra of Hydrogen*, *Carbon*, *Oxygen Atoms and Ions*, CRC Series in Evaluated Data in Atomic Physics (Boca Raton: Chemical Rubber).
[52] Melchionna, S., Ciccotti, G., and Holian, B. L., 1993, *Molec. Phys.*, **78,** 533.
[53] Johnson, J. K., Panagiotopoulos, A. Z., and Gubbins, K. E., 1994, *Molec. Phys.*, **81,** 717.
[54] Smith, W. R., and Tříska, B., 1994, *J. chem. Phys.*, **100,** 3019.
[55] Johnson, J. K., 1999, *Adv. chem. Phys.*, **105,** 461.
[56] McQuarrie, D. A., 1976, Statistical Mechanics (New York: Harper).
[57] Kristóf, T., and Liszi, J., 1998, *Molec. Phys.*, **94,** 519.
[58] Ray, J. R., and Graben, H. W., 1986, *Phys. Rev.* A, **34,** 2517.
[59] Smith, W. R., and Lísal, M. L., 2002, *Phys. Rev.* E, **66,** 011104.

NO. OF COPIES	ORGANIZATION
1 (PDF ONLY)	DEFENSE TECHNICAL INFORMATION CTR DTIC OCA 8725 JOHN J KINGMAN RD STE 0944 FORT BELVOIR VA 22060-6218
1	US ARMY RSRCH DEV & ENGRG CMD SYSTEMS OF SYSTEMS INTEGRATION AMSRD SS T 6000 6TH ST STE 100 FORT BELVOIR VA 22060-5608
1	DIRECTOR US ARMY RESEARCH LAB IMNE ALC IMS 2800 POWDER MILL RD ADELPHI MD 20783-1197
3	DIRECTOR US ARMY RESEARCH LAB AMSRD ARL CI OK TL 2800 POWDER MILL RD ADELPHI MD 20783-1197

ABERDEEN PROVING GROUND

1	DIR USARL AMSRD ARL CI OK TP (BLDG 4600)

NO. OF COPIES	ORGANIZATION
	ABERDEEN PROVING GROUND
5	DIR USARL AMSRD ARL WM BD J BRENNAN